Rail Vehicles/Pojazdy Szynowe

www.railvehicles.eu

Characteristics of fuel cells under static and dynamic conditions

Filip **Szwajca** [a, *] , Andrew W. **Berger** [b], Robert **Spalletta** [b], Ireneusz **Pielecha** [a]

[a] *Poznan University of Technology, Faculty of Civil and Transport Engineering, Poland*
[b] *University of Scranton, Department of Physics & Engineering, United States*

Modern internal combustion powertrains are the main source of propulsion for on-road and non-road vehicles. However, they are increasingly being replaced by electric or fuel cell-equipped alternative propulsion systems. The article presents a study of fuel cell characteristics operating under both static and dynamic conditions, with a 1.2 kW fuel cell set with a voltage converter and lead-acid batteries. In the conducted tests, the fuel cell stack's maximum efficiency reached 65%. Load tests (static and dynamic) have indicated higher fuel cell efficiencies when using hybrid operation with a DC/DC converter and battery.

1. Introduction

Environmental protection requires continuous efforts to reduce the adverse impact of transportation means. The transportation propulsion systems are mostly equipped with internal combustion engines as sources of energy. Stringent emission standards are causing traditional internal combustion engines to be increasingly replaced by alternative vehicle propulsion systems. Stage V emission standards for non-road vehicles (especially rail vehicles) were introduced by Regulation 2016/1628 [25], which regulates requirements for gaseous and particulate emissions limits and approval for internal combustion engines for non-road mobile machinery. The regulation replaced Directive 97/68/EC [5].

Automotive and rail vehicles with hybrid propulsion systems are increasingly replacing conventional powertrains. The most widespread hybrid propulsion system combines an internal combustion engine with electric propulsion and batteries (HEV) with diversified energy management systems [3, 17, 26]. The extensive possibilities of hydrogen production and storage [2, 19, 24] also result in hybrid drive systems being equipped with fuel cells, electric motors and batteries (FCHEV) [1, 8, 21]. The aforementioned alternative propulsion systems are used in cars and non-road - rail vehicles [6].

Passenger cars' powertrain systems equipped with fuel cell stacks do not require significant battery power compared to the power of fuel cell stack, since fuel cell stack power is several times greater than battery power [20]. For instance, in the Toyota Mirai II, the ratio of fuel cell stack power to battery power is 4.06:1 (128 kW:31.5 kW) [27, 28]. In the previous generation of this vehicle model, the ratio was 4.47:1 (114:25.5) [16, 27]. The battery capacities of fuel cell powertrains are comparable to those of traditional hybrids equipped with an internal combustion engine [22]. As an example, the battery capacity in the Toyota Mirai II is 1.24 kWh [27]. It means that the fuel cell stack is the vehicle's main power source and the battery is used only under transient fuel cells stack operation and rapid acceleration conditions. Such conditions require a rapid increase in power, which the battery provides.

Rail vehicles may have different powertrain structures. Various power distribution in the propulsion

* Corresponding author: filip.szwajca@put.poznan.pl (F. Szwajca)

system is possible depending on operating conditions. The FC-Li-Bat rail vehicle presented by Ogawa et al. [18] is equipped with a 100 kW PEM fuel cell stack and 360 kW (36 kWh) Li-Ion battery. The 900–600 V fuel cell stack weighs 1650 kg, and the mass of the 604.8 V battery is 1200 kg. One section of the vehicle is equipped with a hydrogen propulsion system, and the other with a battery powertrain. The total weight of such a vehicle is 70 tons [9]. The study by Kang et al. [15] used a fuel cell stack with a useful power of 250 kW and batteries with a 420 kW power. The nominal voltage of the PEM fuel cell was 625 V, and the battery electrical capacity was 662 Ah, which generates 996 kWh of energy at 1459 V [15]. It was found that the highest efficiency of the hybrid system (about 55%) is obtained when the battery state of charge is 73%.

Fragiacomo et al. [8] used a 150 kW fuel cell stack weighing 404 kg in a simulation study of hybrid propulsion in rail vehicles. In addition, Kokam batteries with an electrical capacity of 40 Ah and a single-cell voltage of 3.7 V were used. A total of 15 kWh of energy was obtained. The system worked based on Maxwell ultracapacitors (UCAP, 48 pcs.) with a summary capacity of 63 F and a voltage of 125 V. The highest system efficiency of 48% was obtained using parallel all three elements (FC + B + UCAP).

There are Europe-wide guidelines for hydrogen fuel [23], hydrogen storage and refueling infrastructure [12, 13]. On 21 October 2022, the Regulation of the Minister of Climate and Environment on Detailed Technical Requirements for Hydrogen Stations was published. This regulation implements Directive 2014/94/EU of the European Parliament and the Council of 22 October 2014 on the infrastructure development of alternative fuels [4]. Hydrogen stations should meet the requirements following ISO 19880-1 and PN-EN 17127 [7]. Hydrogen station refueling dispensers should meet the technical requirements of ISO 19880-1, ISO 19880-2 and PN-EN ISO 17268 [11].

The above considerations make it advisable and desirable to work on the study of hydrogen-powered systems. All work on fuel cells contributes to the green development of transportation means and the reduction of harmful exhaust emissions. As a part of the research, an experimental analysis of fuel cell characteristics was undertaken and the results presented in this article. The fuel cell was tested under static and dynamic conditions.

2. Research methodology

2.1. Test stand

A test stand (Fig. 1) with a 1.2 kW hydrogen-powered, air-cooled fuel cell was used to study the static and dynamic characteristics of the fuel cell stack. The Institute of Internal Combustion Engines and powertrains of the Poznan University of Technology owns the system. The station is fitted with 18 or 7.2 Ah lead-acid battery capacities, depending on the circuit connection. In addition to testing the fuel cell stack, the system also enables analysis of battery performance and hybrid cooperation. Moreover is possible to determine the individual system elements efficiency, for example, the voltage converter. The system can be powered by internal or external hydrogen storage. The detailed technical specifications of the bench are given in Table 1.
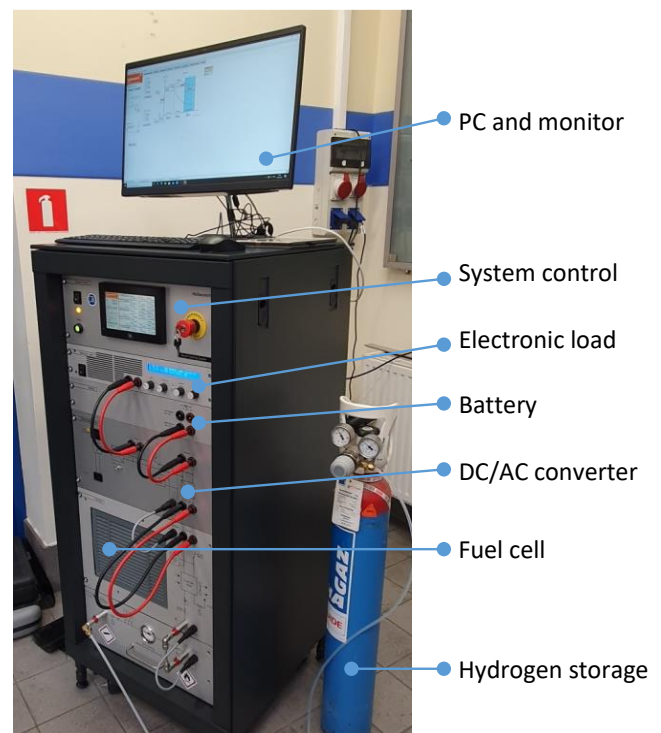

Fig. 1. Heliocentris' Hybrid Energy Lab-System for fuel cell performance analysis

The bench has an electronic load generation system enabling an evaluation of the system in a configuration with a fuel cell stack alone or with a voltage converter and battery. The measurement system includes sensors for analyzing hydrogen flow and temperature. Furthermore, the system provides information about voltage and current on individual components.

The study used a layout with a larger battery capacity of 18 Ah. A schematic diagram of the system is shown in Fig. 2, and the basic equations for analyzing fuel cell operation are included in 2.1.

Applying equations (1)-(5), the efficiency of most components can be determined by analyzing the energy balance in a Sankey diagram (Fig. 3).

Table 1. Technical data of Hybrid Energy Lab-System [10]

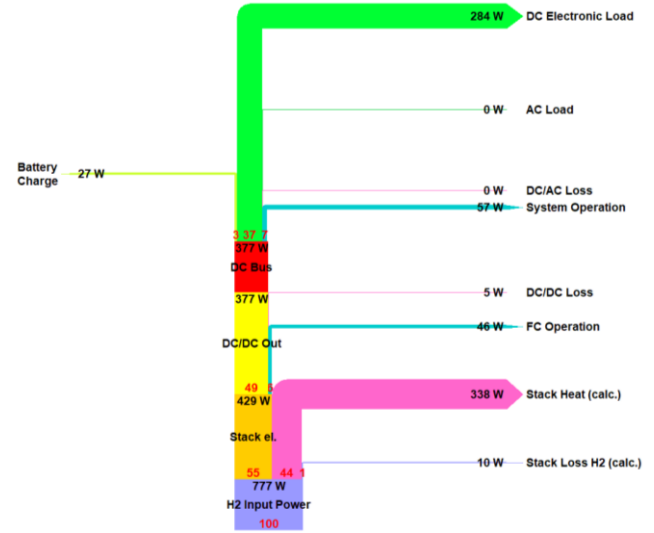| Fuel cell		
Rated output	W	1200
Rated current	A	60
Operating voltage	V	18–36
Hydrogen purity	min	4.0
Permissible H$_2$ inlet pressure	bar	1–15
DC converter		
Max output power	W	1500
Max output current	A$_{DC}$	55
Rated output voltage	V$_{DC}$	24
Output voltage range	V$_{DC}$	21–30
Max input current	A$_{DC}$	60
Input voltage range	V$_{DC}$	18–36
Efficiency	%	96
Inverter		
Continuous output power (50 Hz), 115 VAC (60Hz)	W$_{AC}$	1500
Inlet voltage	V$_{DC}$	21 … 30
Output voltage	V$_{AC}$	230
Efficiency	%	93
Electronic Load Module		
Max. continuous power	W	1200
DC load current	A$_{DC}$	0–85
DC load voltage	V$_{DC}$	0–80
Battery Module		
Battery set 1	lead-acid	24 V, (2 × 12 V), 7.2 Ah
Battery set 2	lead-acid	24 V, (2 × 12 V), 18 Ah

Fig. 3. Example Sankey diagram for power distribution when the system is loaded with a current value of I = 10 A (red data: power percentage of individual systems)
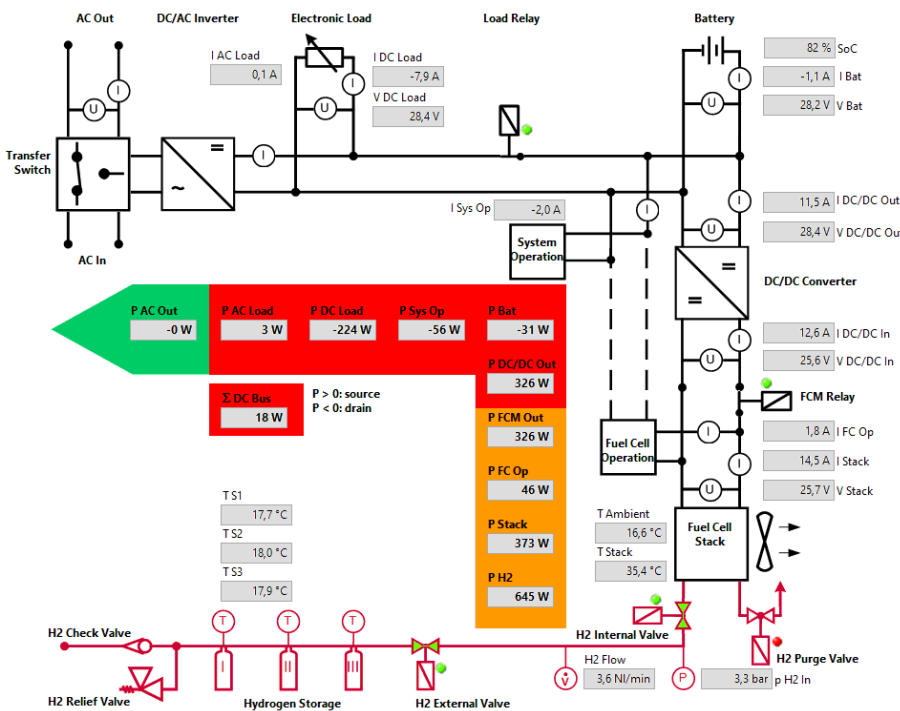
2.1. Scope and plan of research

Fuel cell stack testing was conducted using two profiles:
a) static,
b) dynamic.
and using two load solutions:
- system loads – DC,
- the load of the fuel cell stack – FC.

The extensive analysis included tests for a system containing a voltage converter and a layout without a converter. Static and dynamic load profiles were implemented for both configurations as well.

Fig. 2. Schematic of voltage and current measurements of a fuel cell system with a voltage converter and batteries; according to the schematic symbolism, the equations for further calculations of power and efficiency of the system components are shown

Fuel cell power

$$P_{FC} = U_{FC} \cdot I_{FC} \quad (1)$$

Fuel cell module power

$$P_{FCM} = U_{FC} \cdot (I_{FC} - I_{FC\ Op}) \quad (2)$$

Hydrogen power

$$P_{H_2} = \frac{H_{2fl}}{60} \cdot H_U \ [W] \quad (3)$$

Stack efficiency

$$eta_{FC} = \frac{P_{FC}}{P_{H_2}} \quad (4)$$

Fuel cell module efficiency

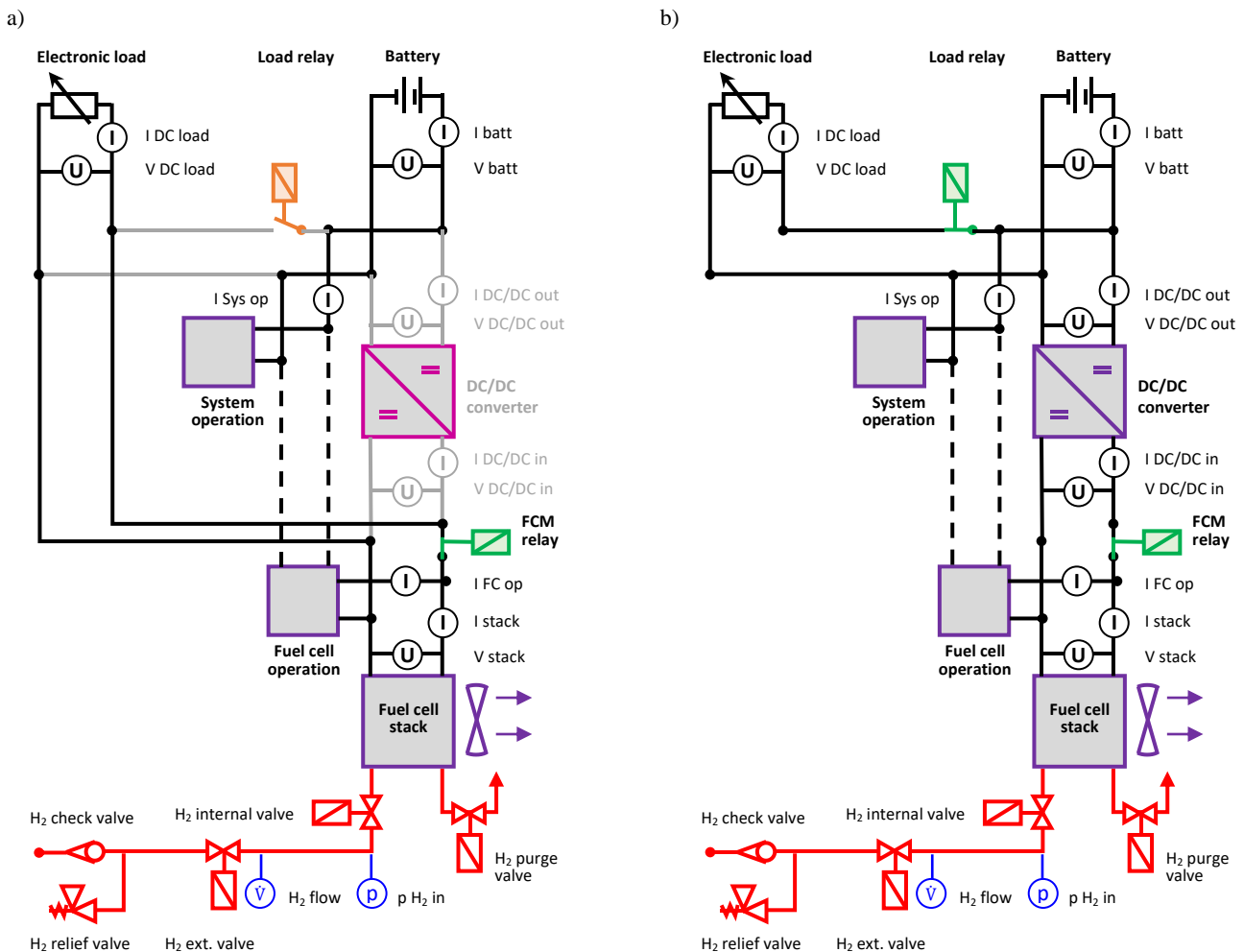$$eta_{FCM} = \frac{P_{FCM}}{P_{H_2}} \quad (5)$$

a)

b)

Fig. 4. Fuel cell test system: a) fuel cell stack tests (designated FC); b) tests of system with DC/DC converter and batteries (designated DC)

The differences in the study of the stack only (Fig. 4a) and the system (Fig. 4b) equipped with a fuel cell relate to their power supply. The cell module uses additional power to supply the system (the so-called operational current).

The differences in the tests carried out on the cell stack and the system with an converter and batteries are shown in Fig. 4.

3. Analysis of fuel cell operation

Fuel cell testing was carried out according to the plan presented in Section 2.1. Analyses were made of the fuel cell stack and system performance under static and dynamic loading (Fig. 5).

Static load refers to the interval-constant load values of the fuel cell and the system. Dynamic load corresponds to the load presented in work [14]. It characterizes the urban dynamometer driving schedule (UDDS) cycle. The internal combustion engine load values were scaled to the fuel cell stack current load.
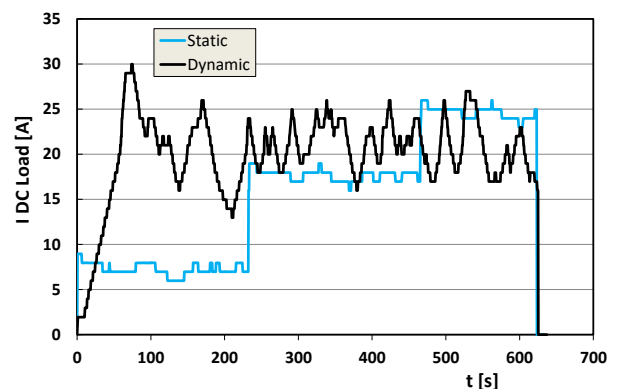

Fig. 5. Profile of static (blue line) and dynamic (black line) loading of the system and fuel cell

The first case analyzed involved loading the fuel cell stack without a voltage converter. This approach made it impossible to charge the battery. The assigned load affected only the fuel cell stack. The second case involved loading the system (including the voltage converter). This approach results in a much smaller load on the fuel cell itself. The static load results are

shown in Fig. 6, which shows that the load on the fuel cell is about 6–8 A less for the system and not the fuel cell stack itself, assuming the same load conditions.
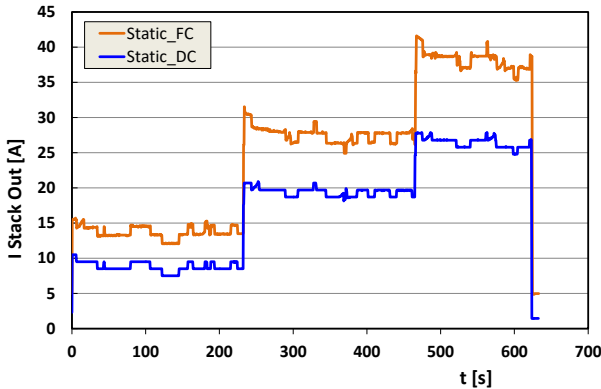

Fig. 6. Responses of the fuel cell (FC) and system (DC) during static load implementation

Analyzing the effects of dynamic loading, a higher current value was obtained for the configuration without a DC/DC converter. High load causes the differences to reach values of more than 15 A. For small changes – the differences are about 10 A (Fig. 7).
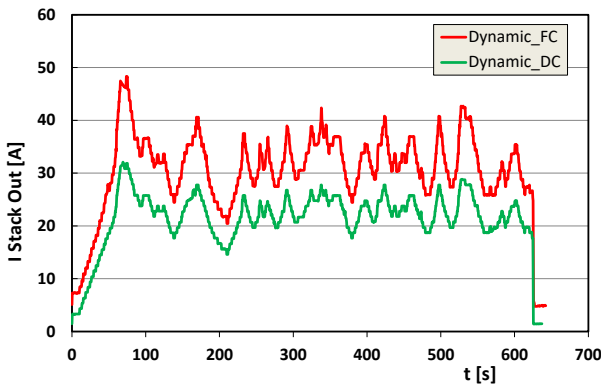

Fig. 7. Responses of the fuel cell (FC) and the system (DC) during dynamic load implementation

Typical voltage-current characteristics are shown in Fig. 8 and 9. Static or dynamic loading slightly "modifies" the performance characteristics of the fuel cell. It can be concluded that in both cases, the operating characteristics are comparable.

In addition, the load on the fuel cell or system itself does not affect changes in characteristics.

The use of equation (3) makes it possible to evaluate the power of hydrogen to power a fuel cell. The characteristics of hydrogen power from current are linear in dependence during both static tests (Fig. 10) and dynamic tests (Fig. 11). The points visible in both figures beyond the area of typical system operation are due to fuel cell stack purge. This means a loss of energy with the hydrogen released into the atmosphere.
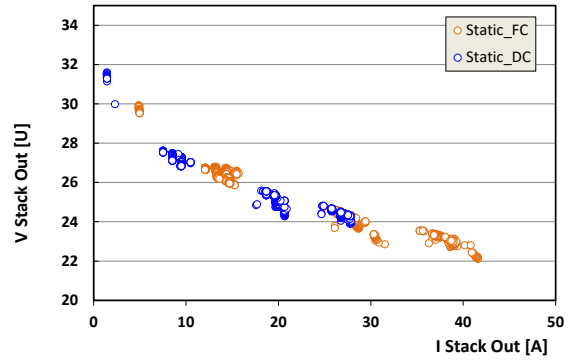

Fig. 8. Current-voltage characteristics of the cell during static load implementation of the fuel cell alone (FC) and the system (DC)
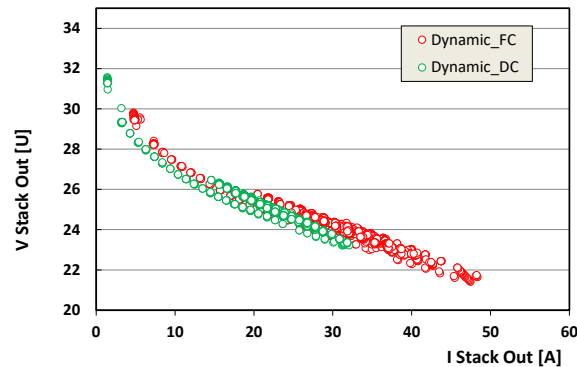

Fig. 9. Current-voltage characteristics of the fuel cell during dynamic load realization of the fuel cell alone (FC) and the system (DC)
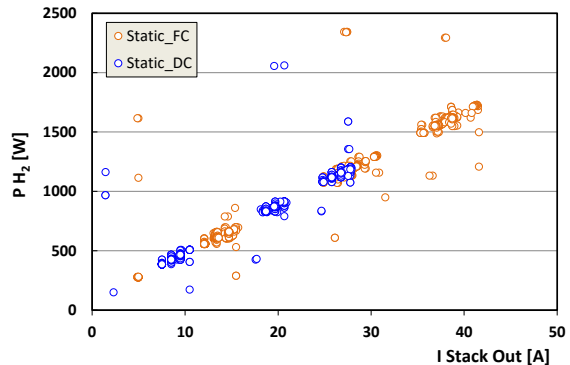

Fig. 10. Hydrogen power characteristics with regard to fuel cell current: during static load realization of the fuel cell itself (FC) and the system (DC)
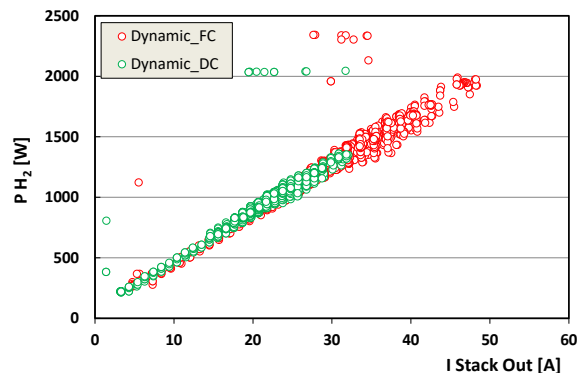

Fig. 11. Hydrogen power characteristics with respect to fuel cell current: during dynamic load realization of the fuel cell itself (FC) and the system (DC)

In both cases (static and dynamic tests), the load on the fuel cell alone results in higher power values than the system.

4. Evaluation of fuel cell performance under static and dynamic conditions

Analysis of typical fuel cell characteristics has made it possible to evaluate further the power obtained from a fuel cell or a system.

Using equations (1) and (2), it is possible to evaluate the power generated by a fuel cell or by a fuel cell system.

The power of the fuel cell system is reduced by the power determined as the product of the fuel cell voltage and the current drawn ($I_{FC\ Op}$). The description of this item ($I_{FC\ Op}$) can be seen in Fig. 3 in the fuel cell area. The determined system power is less than the fuel cell's power under static conditions by about 50 W (Fig. 12).
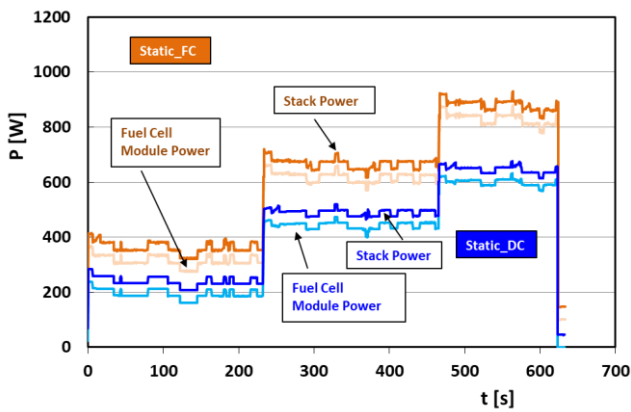

Fig. 12. Static characteristics of the power of the fuel cell (FC) and the system (DC) in relation to the power of the cell itself and the fuel cell module: during the implementation of the dynamic load of the fuel cell itself (FC) and the entire system (DC)

Tests under dynamic conditions show much smaller power differences between the cell and the fuel cell system (Fig. 13). The differences are only a few watts or so. This means that the fuel cell operating losses are much smaller under dynamic conditions than under static loading conditions.

Power differences during static and dynamic tests were determined based on the equation:

$$Delta\ P = P_{FC} - P_{FCM} \qquad (7)$$

Data from static and dynamic tests were used to determine the differences. The results of these analyses are shown in Fig. 14. It shows that the power differences are greater when testing the fuel cell alone. Under dynamic conditions, the differences are larger by about 10%. Under system test conditions, compensation for the use of the converter and the

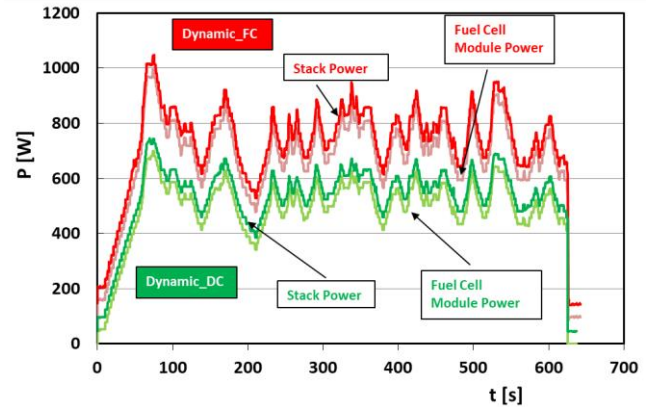battery makes the power differences of the fuel cell and the system the same.

Fig. 13. Dynamic characteristics of the fuel cell (FC) and the system (DC) with respect to the power of the fuel cell alone and the fuel cell system: during the realization of the dynamic load of the fuel cell alone (FC) and the entire system (DC)
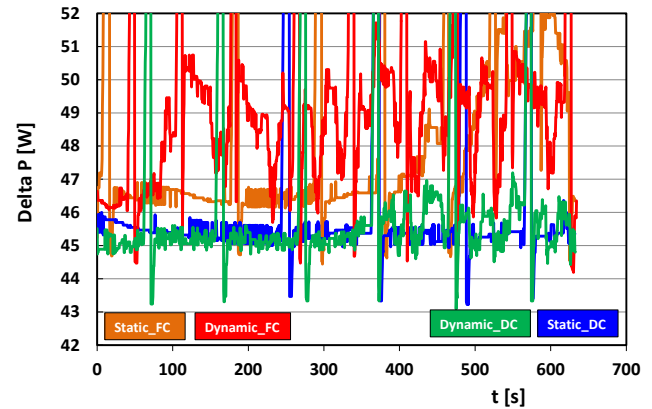

Fig. 14. Power differences under static and dynamic test conditions when evaluating the fuel cell and system

Applying equations (4) and (5), the efficiency values of the fuel cell itself and the system were determined (Fig. 15). Analysis of the equations mentioned above and their components indicates that the efficiency of the fuel cell alone will be higher than that of the system. Such assumptions have also been demonstrated in empirical studies. The operating temperature of the fuel cell during static testing remained about 10°C higher in the initial range of analysis. In the final stage, the value of the difference was about 5°C, also in favour of static testing. The maximum fuel cell efficiency is 60% in the initial stage of testing and decreases (by about 2%) with the course of load changes. The efficiency of the cell stack is about eight percentage points higher than that of the fuel cell system.

Utilizing a voltage converter and its load (Static_DC) indicates lower efficiency values for the fuel cell stack and the system. The fuel cell stack

shows an efficiency of 55–57%, while the fuel cell system shows an efficiency of about 10–15% less.
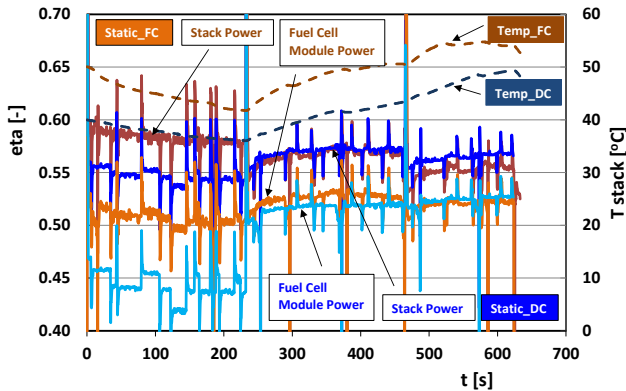

Fig. 15. Analysis of fuel cell and system efficiency during static testing

The timing analysis shown in Fig. 15 indicates that the efficiency of the loaded fuel cell stack is initially greater than the load on the converter and the fuel cell stack. When increasing the load, the efficiency is the same; when the load is very high, the efficiency of the stack is higher while using the voltage converter. This means that high static loads cause a reduction in stack efficiency when the stack is directly loaded. Using a voltage converter (and batteries) to work with the fuel cell is more advantageous.

Dynamic load analysis indicates that loading the fuel cell or voltage converter alone (Fig. 16) allows similar efficiency values – about 57% on average. Dynamic loading conditions indicate smaller efficiency differences between the fuel cell stack and its system.
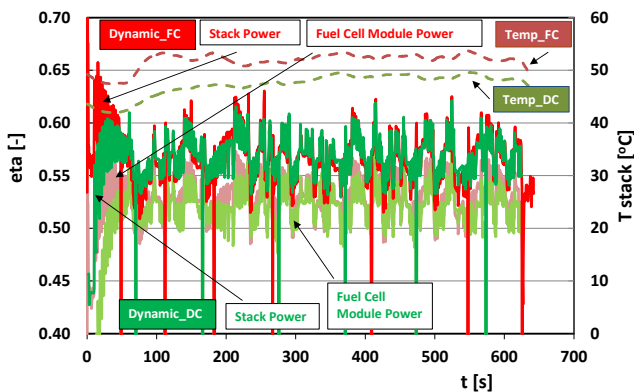

Fig. 16. Analysis of fuel cell and system efficiency during dynamic testing

Analysis of fuel cell efficiency in terms of hydrogen consumption indicates the existence of a local maximum: at about 3 nl/min (n – normal liter per minute), stack efficiency reaches maximum values at static load: 64% (Fig. 17).
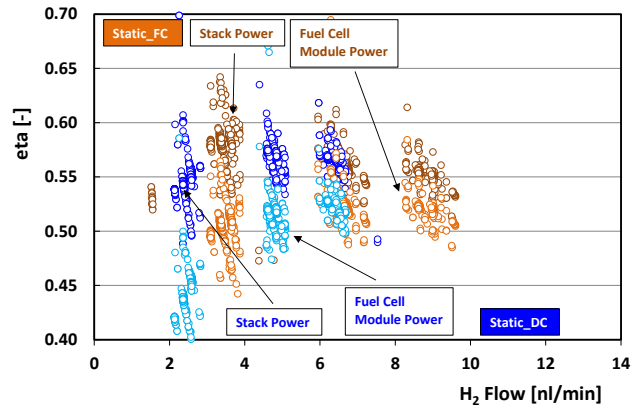

Fig. 17. Evaluation of cell and system efficiency under static conditions based on hydrogen consumption

Similar efficiencies to the previous ones are obtained during dynamic loading analyses (Fig. 18): a maximum fuel cell stack efficiency of 65% was obtained with a hydrogen consumption of about 2–3 nl/min.
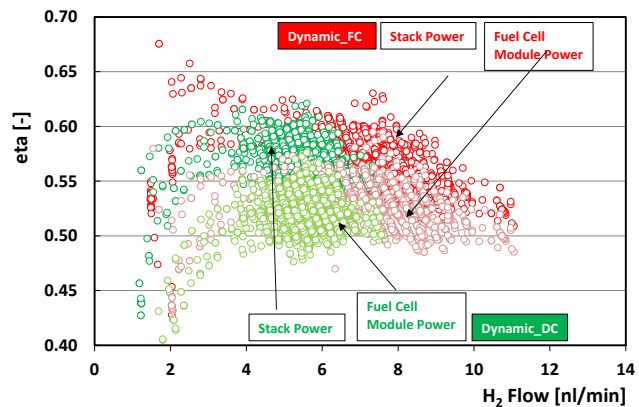

Fig. 18. Evaluation of cell and system efficiency under dynamic conditions based on hydrogen consumption

Summary

In this research, the performance of fuel cells was analyzed under static and dynamic conditions. The two types of load profiles used for the study: reflect the static loads (such as a rail vehicle) and the loads resulting from operation under the conditions of typical passenger vehicle

Detailed analyses indicate the following conclusions in terms of static load:

a) The maximum efficiency of the fuel cell is 60% in the initial phase of testing and decreases (by about 2%) with the course of load changes. The efficiency of the fuel cell stack is about 8 percentage points higher than that of the fuel cell system.

b) The use of a voltage converter and its load (Static_DC) shows lower efficiency values for

the fuel cell stack and the fuel cell system. The fuel cell stack achieves an efficiency of 55–57%, while the fuel cell system achieves an efficiency of about 10–15% less.

c) High static loads reduce the efficiency of the fuel cell stack when it is directly loaded. It is more advantageous to use a voltage converter (and batteries) to work with the fuel cell.

Conclusions on dynamic load of fuel cell:

a) Dynamic load analysis indicates that loading either the fuel cell or the voltage converter alone

results in similar efficiency values – about 57% on average. Dynamic loading conditions indicate smaller efficiency differences between the fuel cell stack and its system.

The maximum efficiency of the fuel cell stack is about 65% and occurs with hydrogen consumption in the range of 2–3 nl/min, which is 20–30% of the maximum hydrogen consumption during the conducted tests. The minimum efficiency of the fuel cell stack (regardless of static or dynamic tests) is not less than 40%.

Nomenclature

B battery
DC system loads
DC/AC direct current/alternating current
eta_{FC} stack efficiency
eta_{FCM} fuel cell module efficiency
FC fuel cell
FCHEV fuel cells hybrid electric vehicles
FCM fuel cell module
FC_{Op} fuel cell operating
fl flow
H_2 hydrogen
H_U hydrogen heating value
HEV hybrid electric vehicles
I current

Li-Ion lithium-ion battery
p pressure
$p_{H2\ in}$ hydrogen pressure inlet
PEM proton-exchange membrane
P_{FC} fuel cell power
P_{FCM} fuel cell module power
P_{H2} hydrogen power
Stage V emission standards for non-road vehicles
U voltage
UCAP ultracapacitor
UDDS urban dynamometer driving schedule cycle
t time
T temperature

Bibliography

[1] Al-Hamed KHM, Dincer I. A novel integrated solid-oxide fuel cell powering system for clean rail applications. Energ Convers Manage. 2020;(205):112327. https://doi.org/10.1016/j.enconman.2019.112327

[2] Böhm M, Del Rey AF, Pagenkopf J, Varela M, Herwartz-Polster S, Calderon BN. Review and comparison of worldwide hydrogen activities in the rail sector with special focus on on-board storage and refueling technologies. Int J Hydrogen Energ. 2022;47(89):38003-38017. https://doi.org/10.1016/j.ijhydene.2022.08.279

[3] Cipek M, Pavković D, Kljaić Z, Mlinarić TJ. Assessment of battery-hybrid diesel-electric locomotive fuel savings and emission reduction potentials based on a realistic mountainous rail route. Energy. 2019;(173):1154-1171. https://doi.org/10.1016/j.energy.2019.02.144

[4] Directive 2014/94/EU of the European Parliament and of the Council of 22 October 2014 on the deployment of alternative fuels infrastructure Text with EEA relevance. European Parliament, Council of the European Union. 22.11.2014. https://eur-lex.europa.eu

[5] Directive 97/68/EC of the European Parliament and of the Council of 16 December 1997 on the approximation of the laws of the Member States relating to measures against the emission of gaseous and particu-

late pollutants from internal combustion engines to be installed in non-road mobile machinery. https://eur-lex.europa.eu/

[6] Durzyński Z. Hydrogen-powered drives of the rail vehicles (part 1). Rail Vehicles/Pojazdy Szynowe. 2021;(2):29-40. https://doi.org/10.53502/RAIL-139980

[7] EN 17127:2020. Outdoor hydrogen refuelling points dispensing gaseous hydrogen and incorporating filling protocols. https://standards.iteh.ai/

[8] Fragiacomo P, Francesco P. Energy performance of a fuel cell hybrid system for rail vehicle propulsion. Enrgy Proced. 2017;(126):1051-1058. https://doi.org/10.1016/j.egypro.2017.08.312

[9] Furuya T, Ogawa K, Yamamoto T. Drive control for fuel cells and lithium ion battery hybrid railway vehicle. 2009 IEEE Vehicle Power. 2009:86-91. https://doi.org/10.1109/VPPC.2009.5289867

[10] Hybrid Energy Lab. Instruction Heliocentris Academia GmbH. 2016. http://www.heliocentris.com

[11] ISO 17268:2020. Gaseous hydrogen land vehicle refuelling connection devices. https://www.iso.org/standard/68442.html

[12] ISO 19880-1:2020. Gaseous hydrogen – Fuelling stations – Part 1: General requirements. https://www.iso.org/standard/71940.html

[13] ISO/DIS 19880-2. Gaseous hydrogen — Fueling stations — Part 2: Dispensers. https://www.iso.org

[14] Kandidayeni M, Chaoui H, Boulon L, Kelouwani S, Trovão JPF. Online system identification of a fuel cell stack with guaranteed stability for energy management applications. IEEE T Energy Conver. 2021;36(4): 2714-2723.
https://doi.org/10.1109/TEC.2021.3063701

[15] Kang J, Guo Y, Liu J. Rule-based energy management strategies for a fuel cell-battery hybrid locomotive. 2020 IEEE 4th C Energ Internet Energ Syst Integr. (EI2). 2020:45-50.
https://doi.org/10.1109/EI250167.2020.9346652

[16] Konno N, Mizuno S, Nakaji H, Ishikawa Y. Development of compact and high-performance fuel cell stack. SAE I J-Alternat Powertr. 2015;4(1):123-129.
https://doi.org/10.4271/2015-01-1175

[17] Lü X, Li S, He X, Xie C, He S, Xu Y. et al. Hybrid electric vehicles: A review of energy management strategies based on model predictive control. J Energ Storage. 2022;(56):106112.
https://doi.org/10.1016/j.est.2022.106112

[18] Ogawa K, Yamamoto T, Hasegawa H, Furuya T. Development of the fuel-cell/battery hybrid railway vehicle. 2009 IEEE Vehicle Power. 2009:1730-1735.
https://doi.org/10.1109/VPPC.2009.5289693

[19] Papadias DD, Peng J-K, Ahluwalia RK. Hydrogen carriers: Production, transmission, decomposition, and storage. Int J Hydrogen Energ. 2021;46(47):24169-24189. https://doi.org/10.1016/j.ijhydene.2021.05.002

[20] Pielecha I. Modeling of fuel cells characteristics in relation to real driving conditions of FCHEV vehicles. Energies. 2022;(15):6753.
https://doi.org/10.3390/en15186753

[21] Pielecha I, Engelmann D, Czerwinski J, Merkisz J. Use of hydrogen fuel in drive systems of rail vehicles. Rail Vehicles/Pojazdy Szynowe. 2022;(1-2):10-19.
https://doi.org/10.53502/RAIL-147725

[22] Pielecha I, Szałek A, Tchorek G. Two generations of hydrogen powertrain—an analysis of the operational indicators in real driving conditions (RDC). Energies. 2022;(15):4734. https://doi.org/10.3390/en15134734

[23] PN-EN 17124:2022-08. Hydrogen fuel – Product specification and quality assurance for hydrogen refuelling points dispensing gaseous hydrogen – Proton exchange membrane (PEM) fuel cell applications for vehicles.

[24] Rasul MG, Hazrat MA, Sattar MA, Jahirul MI, Shearer MJ, The future of hydrogen: Challenges on production, storage and applications. Energ Convers Manage. 2022;(272):116326.
https://doi.org/10.1016/j.enconman.2022.116326

[25] Regulation (EU) 2016/1628 of the European Parliament and of the Council of 14 September 2016 on requirements relating to gaseous and particulate pollutant emission limits and type-approval for internal combustion engines for non-road mobile machinery, amending Regulations (EU) No 1024/2012 and (EU) No 167/2013, and amending and repealing Directive 97/68/EC (Text with EEA relevance). https://eur-lex.europa.eu/

[26] Seyam S, Dincer I, Agelin-Chaab M. Exergetic, exergoeconomic and exergoenvironmental analyses of a hybrid combined locomotive powering system for rail transportation. Energ Convers Manage. 2021;(245): 114619.
https://doi.org/10.1016/j.enconman.2021.114619

[27] Toyota Mirai. Available online: techdoc-toyota.com (accessed on 16.11.2022).

[28] Yoshizumi T, Kubo H, Okumura M. Development of high-performance FC stack for the new MIRAI. SAE Technical Paper 2021-01-0740, 2021.
https://doi.org/10.4271/2021-01-0740